Characterization of mortar-timber and timber-timber cyclic friction in timber floor connections of masonry buildings

João P. Almeida [1)], Katrin Beyer [2)], Roland Brunner [3)], and Thomas Wenk [4)]

Abstract

The seismic performance of buildings depends critically on the stiffness and strength of storey diaphragms. Whilst for modern reinforced concrete or steel structures the connection between floors and lateral resisting members is often assumed as monolithic, timber floors and ceilings in masonry buildings are susceptible to sliding in their supports. In fact, the anchorage of timber beams in masonry walls and intermediate supports relies partly or totally on a frictional type of resisting mechanism. The present work contributes to characterize this behaviour by presenting the results of an extensive experimental programme with cyclic friction triplet tests between mortar and timber units, and between timber and timber units. These were produced to be representative of connection typologies characteristic of pre-modern and contemporary construction periods. Each test was performed under a constant level of contact pressure, which was increased throughout each series to cover a range of normal forces foreseeable in building connections. Other aspects are also discussed, such as the influence of cumulative loading or velocity. The experimental data is made available for public use (doi.org/10.5281/zenodo.3348328).

Keywords: *Timber, Floors, Friction Coefficient, Kinetic Friction, Seismic Engineering, Masonry Walls.*

1) Formerly: Earthquake Engineering and Structural Dynamics Laboratory (EESD), School of Architecture, Civil and Environmental Engineering (ENAC), École Polytechnique Fédérale de Lausanne (EPFL), Switzerland.
EPFL ENAC IIC EESD, Station 18, CH – 1015 Lausanne
Currently: Institute of Mechanics, Materials and Civil Engineering, UCLouvain, Belgium.
Place du Levant 1 L5.05.01, B 1348 Louvain-la-Neuve, Belgium.
joao.almeida@uclouvain.be

2) Earthquake Engineering and Structural Dynamics Laboratory (EESD), School of Architecture, Civil and Environmental Engineering (ENAC), École Polytechnique Fédérale de Lausanne (EPFL), Switzerland.
EPFL ENAC IIC EESD, Station 18, CH – 1015 Lausanne
katrin.beyer@epfl.ch

3) Lignum, Holzwirtschaft Schweiz, Mühlebachstrasse 8, CH-8008 Zürich
roland.brunner@lignum.ch

4) Gehrenholz 2h, CH-8055 Zürich
wenk@member-sia.ch

1 Introduction

Old masonry buildings, as constructed during several centuries, and many modern ones as well, are composed of masonry walls with timber floors and ceilings. The ideal type of behaviour of these structures, when subjected to seismic action, is the so-called 'box-type' response [1]. It aims at making up for the usual low resistance of walls to out-of-plane loading with their much higher resistance to in-plane loads. Such objective can only be accomplished by an efficient distribution of floor diaphragm inertial forces between the supports, without which a global structural response cannot be guaranteed and local out-of-plane failures of walls can take place. This force distribution depends on the in-plane timber floor stiffness, for which significant research work has been done

[2,3], and on the ability of the connections to transmit those diaphragm forces to the wall. Effective connections are thus fundamental to prevent walls from behaving independently and possibly failing through an out-of-plane mechanism. Floor timber beams can be supported by other perpendicular timber trimmer beams, see Fig. 1, or directly by the masonry walls. This connection behaviour usually depends heavily on a frictional type of mechanism. Previous research addressed the friction of dry joints between stones [4], of a crack within a brick [5], between masonry mortar [6], between various timber products [7–11], and between timber and other materials [12–14]. The objective of this paper is to investigate the cyclic friction of timber-timber and mortar-timber joints that are present in old and new masonry buildings with timber floors.

It should be noted that the transfer of inertial forces to the walls can also occur through the two following additional mechanisms: (i) a physical anchoring system, e.g. tie rods, if present, or (ii) through pushing of the timber beam extremities against the masonry wall. Up to values of relative beam-wall displacements where both mechanisms are typically activated, the friction mechanism plays the fundamental load-transfer role. In other words, the characterization of the latter appears to be particularly important for regions of low to medium seismicity, such as Switzerland. Therefore, limit states corresponding to local wall failure due to beam pounding or anchorage system punching are not considered. Moreover, beam unseating is also not accounted for: assuming a worse-case scenario, with small seating lengths (e.g., 10 cm) and (unrealistic) synchronous out-of-phase displacements of the two opposite walls spanned by the beam, unseating is obtained only for very large inter-storey drifts (≈ 0.05 m / 3 m = 1.7%), well above the displacement capacity of typical masonry walls.

According to the review work by Platzgummer et al. [15], floor systems (apart from the roof) remained approximately the same from the Middle Ages (9th century) to the end of the Early Modern Period (early 19th century). In the basements, the timber floor beams, which appear to have been more commonly used than vaults, were typically supported by stone consoles. Sometimes, a trimmer beam running parallel to the wall was placed between consoles and floor beams in order to redistribute the load among the consoles, see Fig. 1. Above ground, the floor beams were either placed directly onto the wall (i.e., stone or mortar) or again on a trimmer beam. This wall support could be of the form of a slot left during the erection of the walls or typically created by the reduction of the wall thickness at each storey, creating a small pedestal on which beams were placed. The same source mentions support lengths of 10-15 cm. It is noted that the floor beams have a fibre (grain) orientation that is perpendicular to that of the support trimmer beam. During the Baroque period, another typical constructional detail is the use of timber columns supporting a large beam that serves as intermediate support for the floor beams spanning between two masonry walls. Also in this situation the fibre orientation of the large support beam is orthogonal to the floor beams.

Fig. 1. Timber floor beams resting on perpendicular trimmer beams on stone consoles.

The present study contributes to a better understanding and characterization of mortar-timber and timber-timber friction in timber floor connections of masonry buildings. Friction is a surface force that restrains the rolling or sliding motion of bodies that are in contact and originates in irregularities and roughness of the surfaces of those bodies. Molecular attraction between the contact surfaces may cause microwelding that must be broken to start sliding [8]. Three classical generalizations regarding friction are that: (1) the friction force $F_{friction}$ is independent of the normal area of contact, (2) the friction force $F_{friction}$ is proportional to the normal (contact) force $N_{contact}$, (3) the friction coefficient $\mu = F_{friction} / N_{contact}$ is practically independent of the sliding speed [12]. However, past experimental tests have shown that some of these hypotheses do not apply for all ranges of conditions. Friction generally depends on the type of surfaces in contact and can be classified into dry, fluid lubricated, skin and internal friction [16].

It is surprising to observe that, although wood is a widely used material, and despite an initial boost on investigations during the 1950s and 1960s [12,17], limited research on its frictional properties can be found.

The type of wood friction investigated in the current study is dry friction, for which friction coefficients depend primarily on moisture content and surface roughness. **Moisture content** increases friction coefficients up to the point of fibre saturation. Furthermore, it was shown that the kinetic friction decreases relevantly with increasing velocity [18]. Svensson et al. [13] also reported that, at high sliding velocity, the coefficient of friction between spruce wood and smooth steel depends linearly on the moisture contents of the specimens. Nonetheless, for the small range of typical moisture contents in connections inside masonry buildings this effect is minimal and therefore it is not addressed in the current study. **Roughness**, on the other hand, relates with the surface protuberances, which keep elements in contact and determine the actual contact area. The rougher the surface, the larger the number of protuberances. When the pressure between the contact surfaces increases, the actual area in contact also grows as protuberances are deformed [8]. The investigation by Chen et al. [9] showed that the surface roughness of different wood floors influenced significantly the friction coefficients. More recently, Xu et al. [10] confirmed that the frictional properties of wooden materials were affected by both surface roughness and hardness. The former was measured with a stylus-type profile meter along an evaluation-length of 12.5 mm, and evaluated based on the arithmetic mean deviation of the profile (R_a) and maximum height of the profile (R_z). The wood friction coefficients increased with R_a, capped at a certain value for wood-based panel units.

The maximum shear force that can be developed before the bodies start sliding relative to each other is called **static friction** force. As the applied force is increased and exceeds the static friction force, the two bodies start moving relative to each other and the resisting force drops to the level of **kinetic friction**. It is fundamental to characterize both the static and the kinetic friction coefficients to better understand earthquake response. For any two surfaces in contact, the static friction coefficient μ_{static} is usually higher than the kinetic friction coefficient $\mu_{kinetic}$. Meng et al. [11] indicate that the ratios of kinetic frictional coefficients to static frictional coefficients range from 0.6 to 0.9. Another recent study also indicated that the variability in the static friction properties is larger, in particular for the first load cycle [7]. It is noted that, if uniform stresses within contact surfaces are assumed, the friction coefficient can also be expressed as the ratio of the shear stress (τ) to normal stress (σ).

Some aspects have been thought to possibly affect the surface roughness and friction coefficients, namely: **wood species**, **fibre orientation**, **contact pressure**, **loading velocity**, **cumulative displacement**, and **temperature**. The study of the influence of each aspect ultimately requires experimental testing. However, although the first studies on wood-wood friction were carried out many decades ago [12], there is not a large body of literature on the topic. Most research focuses on friction between timber and other materials. To further complicate matters, existing research shows a wide range of values for the friction coefficient between wood and wood, varying between 0.15-0.2 and 0.7-0.8 depending on the study.

In the course of an experimental program to study the influence of different variables affecting friction between wood and steel, McKenzie and Karpovich [12] also briefly investigated the friction properties between wood and wood. They reported a reduction of the kinetic friction coefficient with sliding speed (relatively high speeds were considered, up to 55 mm/s), although it was clearly more apparent for wet conditions than with low moisture contents (12%). More recently, when studying Oriented Strand Board (OSB)-OSB friction and OSB-GLT (Glued Laminated Timber) friction, Steiger et al. [7] confirmed that the loading velocity affects the friction coefficient: the higher the loading velocity the lower the friction coefficient. However, this effect seems to be rather small.

Regarding fibre orientation, Aira et al. [8] analysed the static and kinetic friction coefficients of Scots pine between transverse surfaces sliding perpendicular to the grain and radial surfaces sliding parallel to grain. Results of the experiment shows that the coefficients of friction between transverse surfaces [$\mu_{static} = 0.24$; $\mu_{kinetic} = 0.17$] were about twice of the coefficients of friction between radial surfaces [$\mu_{static} = 0.12$; $\mu_{kinetic} = 0.08$]. The studies by Meng et al. [11] and Bejo et al. [19] also indicated that frictional coefficients perpendicular to the grain of timber are larger than those parallel to the grain. The tests by Steiger et al. [7] indicated that, on average, the friction perpendicular to the grain is about 30% larger than parallel to grain, noting that this influence is consistent with the values proposed by Niemz [20]. Lastly, the tests by Xu et al. [10] indicate that the friction coefficient was maximized when the grain directions of two wood specimens were perpendicular to the sliding direction or perpendicular to each other.

Past tests where the influence of contact pressure was analysed were inconclusive. Murase [21], based on tests with low contact pressures (0.002 to 0.06 MPa), concluded that the friction coefficient between two pieces of hemlock with planed surfaces was found to be independent on the level of contact pressure. On the other hand, Bejo et al. [19] obtained, from research with products derived from wood (Laminated Strand Lumber and Laminated Veneer Lumber), a nonlinear decaying trend of the friction coefficients with increasing contact pressure between adjacent surfaces. This disagreement can perhaps be explained by differences in the range of applied contact pressure and specific features of the wood species tested. More recently, Steiger et al. [7] studied wood-wood friction with contact pressures varying between 0.05 MPa and 1 MPa. They concluded that the friction coefficient was only marginally influenced by the applied levels of compressive stress. It is noted that, as estimated in Table 1 below, 0.5 MPa is an upper bound limit of the contact pressure for friction interfaces between timber beams or beam-wall connections, but it is expected that the vast majority of connections are subjected to normal pressures below 0.25-0.3 MPa.

Finally, it is also of importance for seismic applications to refer that one recent study analysed the influence of the cumulative displacement on the cyclic frictional behaviour. It was shown that the friction coefficients between OSB-OSB and OSB-GLT decrease with increasing cumulative displacement, which the authors attributed to a grinding of the contact surface [7]. However, after a cumulative displacement of about 100 mm the friction coefficients remained constant. Static friction coefficients for load cycles after a cumulative displacement of 100 mm are about half of the static friction coefficient of the first load cycle. The influence of the cumulative displacement on the kinetic friction coefficient is smaller (10% to 20%) [7]. The same authors also noted that peak shear stresses identified in opposing directions are usually slightly different.

The next sections describe an experimental programme to characterize the influence of the most relevant and insufficiently tested parameters on mortar-timber and timber-timber cyclic friction behaviour, considering the above literature review. These parameters were selected in the context of the seismic response of timber floor to wall connections in masonry buildings, and include: contact pressure, roughness, effect of cumulative loading, loading velocity, and fibre orientation.

2 Experimental Program

2.1 Timber floor typologies

Concerning timber floor typologies, the authors consider a division between a pre-modern period, starting from the Middle Ages, and a contemporary period (herein also called modern era), starting around the early-mid XX century. This separation was defined based on an extensive number of visits to buildings in Switzerland and discussion with practitioners and construction specialists, with Table 1 summarising these differences. It is expected that these values also hold for neighbouring regions in the wider central Europe. The table also shows computed lower and upper bounds of the contact (transverse) pressure. When live loads are large, the floor beams can bend significantly, which may reduce the contact area due to a possible uplift of the beam extremities embedded in the wall. In-plane floor distortion may lead up to a similar effect.

2.2 Test setup and loading

Friction is characterized through cyclic tests that resort to a new test setup, described below. Previous research on friction has used different test setups [4], although they admittedly fail to reproduce an uniform distribution of normal and shear stresses along the contact surfaces [22]. Efforts have been made to minimize undesired effects associated with the appearance of bending, which is responsible for variations of normal stresses in the joints [23]. The triplet test has been adopted as the standard test in Europe. Recently, Steiger et al. [7] used a test setup where three bodies were pressed together by means of four horizontal steel rods. The two outer bodies remained fixed throughout the test, while the inner one was cycled vertically. Beforehand, the rods applied a pre-compression throughout the joints. The rods' stresses were monitored by measuring the strain in the rods.

The concept for the current test setup is similar, except that the contact force was actively controlled throughout the test [6]. Two perpendicular actuators were used, which enable the simultaneous application of a horizontal (contact) force and cyclic vertical (shear) displacements. The test setup consists of a three-block symmetric system where each test unit is placed in a metal bracket. The left block is fixed to a base plate, the central block is supported by a top roller connected to the vertical actuator, and the right block is supported by a roller connected to the base plate. The central metal bracket consists of a frame around the test unit, therefore allowing for both surfaces of the central unit to be in contact with the left and right outer units. The thickness of the central unit obviously needs to be larger than that of the frame. The horizontal actuator pushes leftwards against the back of the right metal bracket, therefore putting the three units into contact. Once placed in these metal brackets for the first time, the test units are pushed against each other with a low value of compression force (around 100 N, which corresponds to approximately 0.008 MPa), such that the test unit surfaces adjust themselves to each other. One can think of this operation as emulating a beam self-weight adjustment to its own supports. This equilibrium position of each unit is then preserved by fixing it to the corresponding metal bracket through a vertically-adjustable steel piece, tightened by two screws on threaded bars that compress each unit downwards. Fig. 2 shows a close-up view and a sketch of the test setup with the three units before and after contact, respectively Fig. 2(a) and Fig. 2 (b).

For each test, a defined value of horizontal compression (contact) force, $N_{contact}$, is applied and kept constant throughout the test. Simultaneously, a history of cyclic shear displacements is applied by the vertical actuator according to the indications in the Section 2.3. The friction force, $F_{friction}$, is recorded by the vertical actuator while the vertical displacement is measured with respect to the base plate by two linear variable differential transformers (LVDTs) placed on each side of the central block metal frame. In other words, the values of friction displacement indicated correspond to the relative displacement between the central unit and the two outer units. The vertical displacement shown in the test results corresponds to the average of these two LVDT measurements. The difference between both was seen to be very small, which proves that the central metal frame stiffness against distortion deformations was adequate. The horizontal actuator displacement was also recorded. Data acquisition was performed at a rate of 5 Hz.

Table 1. Characterization of timber floor construction and loading in the pre-modern (before early-mid XX century) and contemporary periods.

	Pre-modern period	**Contemporary period**
Timber type	beams: spruce or pine; girders: spruce or oak	beams: spruce or pine; no girders
Span width of beams (l)	$l \approx 3$ to 4 m	$l \approx 4$ to 6 m
Spacing of beams (s)	$s \approx 1$ m	$s \approx 0.6$ m (0.6 m is a carpenter rule, even today)
Cross section of beams *(h: height; b: width)*	$b \approx 0.15$ to 0.3 m $h \approx 0.15$ to 0.3 m	$h / b \approx 2$ and $l / h \approx 20$ (these ratios are carpenter rules)
Surface treatment	hacked	sawed without treatment or planed
Embedment length in walls (l_e)	$l_e \approx 0.1$ to 0.2 m (or half the wall thickness)	$l_e \approx 0.1$ to 0.15 m
Floor construction	50 to 80 mm thick spruce or pine boards on top of beams, bottom open or with various types of insulation	25 to 35 mm thick spruce or pine boards on top of beams, bottom: rush mat with gypsum
Dead load of floor slab	without insulation: 0.4 to 0.6 kN/m^2 with insulation: 0.6 to 2.0 kN/m^2	without insulation: 0.5 to 1.0 kN/m^2 with insulation: 1.0 to 2.0 kN/m^2
Live load on floor slab	$\leq 0.3 \times 2$ kN/m^2 = 0.6 kN/m^2	$\leq 0.3 \times 2$ kN/m^2 = 0.6 kN/m^2
Vertical reaction force on simply supported beam considering no load transfer between neighbouring beams	0.6 to 5.2 kN	0.6 to 4.7 kN
Transverse pressure on beam over embedment wall length	0.01 to 0.35 MPa	0.027 to 0.47 MPa

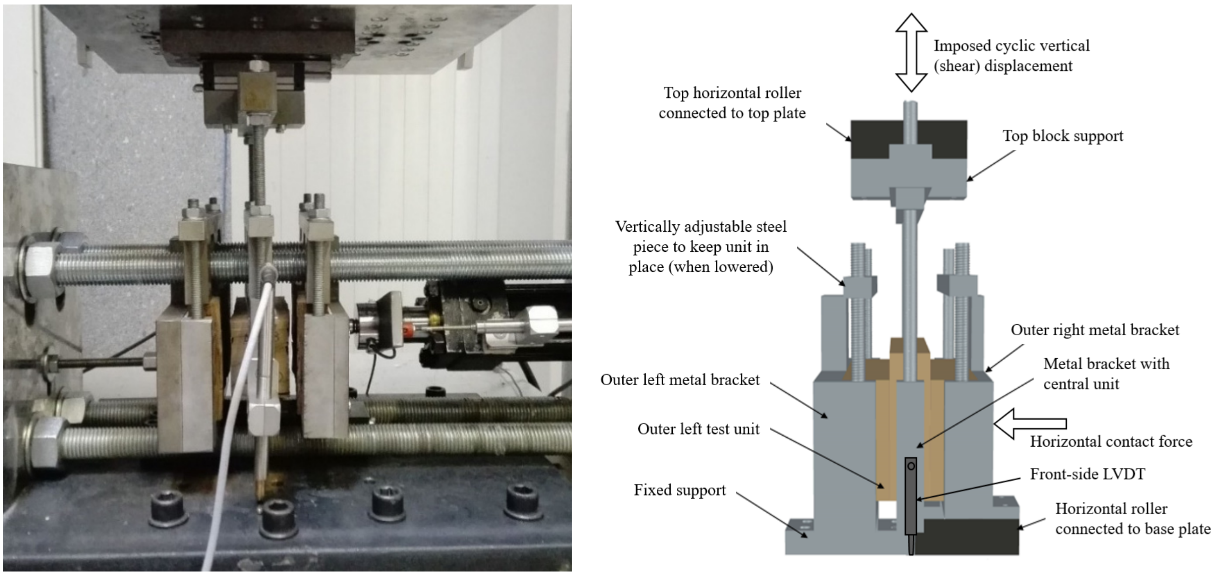

(a) (b)

Fig. 2. Test setup with the three test units not yet in contact: (a) Close-up view; (b) Sketch.

2.3 Test units and loading protocol

Timber beams used in actual construction during the two abovementioned periods were purchased from the Swiss wood trading company *Atlas Holz AG*. One is an oak specimen, while the other two are spruce. Slices were cut out from the beam outer surface to fit the geometrical constraints of the test setup metal brackets described above. The units for the central block were obtained after gluing together two outer surfaces. Silver fir was considered for modern construction with two different types of surface treatment, and therefore different roughness: planed surface (appearance class N, GL24h), as well as rough sawn surface (appearance class N, C24) [24–26]. The moisture content in the test units was estimated to vary between 8 % and 12 %, which is judged representative of typical connections inside masonry buildings.

Wood is an orthotropic material, and therefore the degree of roughness can vary between the three principal planes: perpendicular to the grain, or parallel (radial or tangential). Friction coefficients can be studied and will in general depend on the type of surfaces in contact as well as on the relative direction of sliding. Additionally, the cuts along the surfaces parallel to the grain give rise to a slight orientation of the roughness (this effect is commonly called 'with the woodgrain and against the woodgrain'), which also influences friction values [8]. Although time constraints do not allow addressing all possible combinations of this parameter, an original intention of the present study was also to assess its influence for the most common connections.

Two types of mortar were considered. One, weaker, considered representative of historic buildings in the Middle Ages, was prepared using an approximate 1:2 ratio of hydraulic lime to sand. The other, stronger, representative of modern construction, was produced without aggregates. It will be discussed later that such division is somewhat artificial.

The length and width of the central test units (around 175 mm × 70 mm) were cut smaller than the corresponding dimensions of the outer test units (around 190 mm × 95 mm) in order to try to keep a constant friction area during the tests, which is used to compute the contact pressure. However, it was observed that the contact between the test units mainly occurs in small localized areas within the units' surface, which are not necessarily correlated with the apparent overall contact area. This was particularly evident for the very rough test units of the pre-modern period.

Standards for shear tests on timber structures do not specify compressive stresses for timber specimens. Therefore, estimates of lower and upper bounds for the contact force were obtained in Table 1. Tests were carried out for different levels of contact stress according to the range therein identified. For the purpose of the comparative analyses carried out in this study, the normal contact pressure σ was divided in three groups: 'Low contact pressure' for $\sigma < 0.1$ MPa, 'Intermediate contact pressure' for 0.1 MPa $< \sigma <$ 0.2 MPa, and 'High contact pressure' for $\sigma >$ 0.2 MPa.

Regarding the imposed cyclic displacement variations, geometrical test setup constraints limited these to ± 1 cm, which is in accordance with other tests [7]. On the other hand, it was observed from preliminary tests that the peak (static) friction could occur for a central-block displacement variation of around 0.5 mm, which is thought to be mainly due to a recoverable deformation of the units outside the steel brackets and not from an actual relative displacement between contacting surfaces of the units. Therefore, ± 1 mm was defined as the smallest cycle amplitude to be applied. The latter seems to be in line with the observations of other authors [7], who note that for load cycles with small amplitudes the identification of the peak value and the residual value is associated with large uncertainties, and therefore recommend load cycles with peak-to-peak amplitudes larger than 3 mm. One final requirement was to limit the testing time of each unit to approximately 1.5 hours (including unit replacement time in the setup), in order to allow testing as many units as possible. The joint consideration of all the above conditions was reflected on the definition of the following cyclic displacement-controlled loading protocol (Fig. 3(a)): ± 1 mm → ± 5 mm → ± 10 mm. This protocol was applied to the large majority of the tests in the current program. Deviations were considered in very specific cases, for instance in a few tests to evaluate the impact of cycle amplitude and number of load cycles (i.e., cumulative cyclic displacement) in the response. The loading velocity was kept equal to 0.1 mm/s.

3 Data Filtering and Characteristic Friction Coefficients

3.1 Initial observations and data filtering

Over 400 cyclic friction tests, organised in series, were performed: mortar-antique timber-mortar (55 tests), mortar-modern timber-mortar (103 tests), antique timber (80 tests), and modern timber (165 tests).The test data are publicly available and free to download from the platform Zenodo, at the following DOI: doi.org/10.5281/zenodo.3348328. Fig. 3(a) shows the evolution of the contact force and the measured vertical (friction) displacements throughout the load stages (LS) of a randomly chosen test with antique timber units, while Fig. 3(b) depicts the corresponding friction coefficient-displacement response. Contact forces commonly expected in actual floor-wall connections, i.e. up to a normal pressure σ of around 0.25 MPa, were chosen for the majority of the tests. However, slightly larger values, within the ranges defined in Table 1, were also explored. In general, an increasing value of the contact force $N_{contact}$ was applied for consecutive tests within each series, as this was one of the main variables investigated.

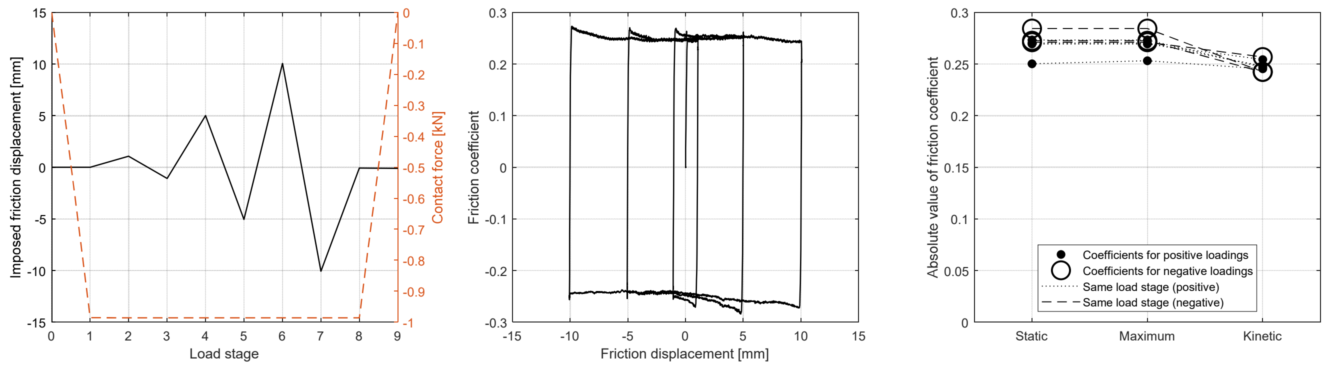

(a) (b) (c)

Fig. 3. Post-processed results of one friction test with antique timber units obtained from a 16th century oak beam ($\sigma \approx 0.08$ MPa).

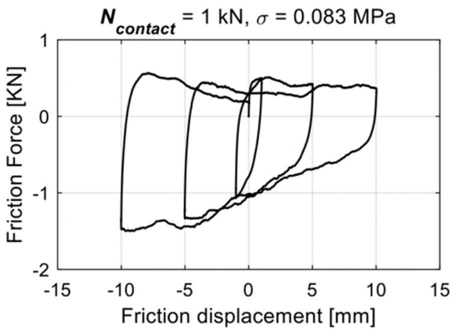

Fig. 4. Example of antique mortar-timber tests that were excluded from the statistical analyses.

The results of each test were checked individually for consistency during and at the end of the experimental programme to filter out unsound data. Only tests depicting a Coulomb-friction type of response were validated. In particular, it was observed that tests performed with units representing antique mortar, described in Section 2.3, did not present a frictional type of behaviour. Fig. 4 shows a result of one example of such antique mortar specimens. The physical explanation is that, even at low horizontal pressures, the mortar units start grinding, breaking up, and reducing into small particles and powder. This effect is very significantly enhanced when the compression force increases. It was hence decided to discard all the series with this friable material from the analyses, as well as test series showing any particular unaccountable feature. The authors consider that the rapid disintegration of antique mortar layers in connections will quickly lead to the contact between the timber beams and the stronger layers underneath, of brick or stone, for which the results corresponding to the modern mortar units can be used as an estimate.

Apart from the cases reported above, a first overall observation is that the specimens showed in general a rather Coulomb-friction-like type of behaviour, as seen in Fig. 3, which is a relevant conclusion for modelling purposes. Moreover, it was observed that the behaviour was less regular for very low values of contact pressure (say, for $\sigma < 0.02$-0.04 MPa), which is attributed to the local heterogeneity of the units' surface. This influence is naturally clearer for the antique timber specimens. Higher contact pressures tend to smooth out this effect. The next paragraph indicates the adopted procedure for the determination of the friction coefficients whereas the following sections present a discussion of the statistical treatment of all filtered data.

3.2 Determination of static, kinetic, and maximum friction coefficients

The friction coefficient μ is directly obtained with the following formula:

$$\mu=\frac{F_{friction}}{2 \times N_{contact}} \tag{1}$$

The factor of two in the denominator is due to the two friction surfaces of the triplet test. As the contact force $N_{contact}$ was kept constant during each test (see Fig. 3(a)), the friction coefficient-displacement curve has necessarily the same shape of the friction force-displacement response. For each semi-cycle in each test, three characteristic values of the friction coefficient were determined.

The maximum shear force transmitted by contact before relative sliding of the bodies is the so-called static friction force [7,8]. The corresponding friction coefficient is the static friction coefficient, which was identified for every semi-cycle in each test as the absolute value of the first local peak upon virgin loading or unloading-reloading after each load stage. While such peak identification can be straightforwardly automated in most cases [27], see for instance Fig. 3(b), there are tests in which a close manual inspection was required.

Additionally, it was also judged important to identify the maximum friction coefficient within two consecutive load stages. The static and the maximum friction coefficients often coincide, as one would expect. However, that is not necessarily always the case. The discrepancy between the static and maximum friction coefficients serves as a measure of how much the behaviour of the present units differs from classical dry friction. Finally, the kinetic friction coefficient was found by averaging the values of the friction coefficients corresponding to the last third of data points between load stages. Fig. 3(c) shows the post-processed values corresponding to the static, maximum, and kinetic coefficients for all semi-cycles in the shown illustrative test.

4 Mortar-Timber Friction

4.1 Mortar-antique timber

Fig. 5 shows the values of the static, maximum and kinetic friction coefficients for all semi-cycles of all tests involving mortar-antique timber units plotted in function of the contact pressure. It shows that the maximum friction coefficient is only slightly larger than the static coefficient, and further that the kinetic coefficient is essentially similar to the static coefficient. Fig. 5 points out a weak correlation between the friction coefficient and the contact pressure in the low pressure range ($\sigma < 0.1$ MPa), beyond which the former remains constant up to significantly large values of the contact pressure. Table 2 confirms this observation, which holds for a range of contact pressures up to around 0.35 MPa and covers most of expected practical cases.

Histograms show that the static, maximum, and kinetic friction coefficients are rather acceptably represented by a normal distribution, confirming a reliable statistical characterization. A summary of the corresponding means and standard deviations is included in Table 2.

Differentiation between the results obtained for the semi-cycles in each loading direction (i.e., for 'positive loading' and 'negative loading' directions) was also performed. Although some randomness is observable among and within individual tests, on average the friction coefficients corresponding to the positive and negative semi-cycles were similar. This was found to be a general conclusion applicable to all tests and therefore no further distinction will be made in the remainder of this study.

The mortar-antique timber tests yielded friction coefficients 10-15 % lower than the mortar-modern sawn timber (i.e., similar to the mortar-modern planed timber, or marginally higher), see Table 2. In other words, although the surface of antique timber units is undoubtedly more uneven and bumpy when compared with modern timber, the increased local roughness of the modern sawn units appears to be a more governing factor. At the same time, the reduced control in the production process of old timber beams over contemporary ones is reflected, as expected, in a slightly higher standard deviation.

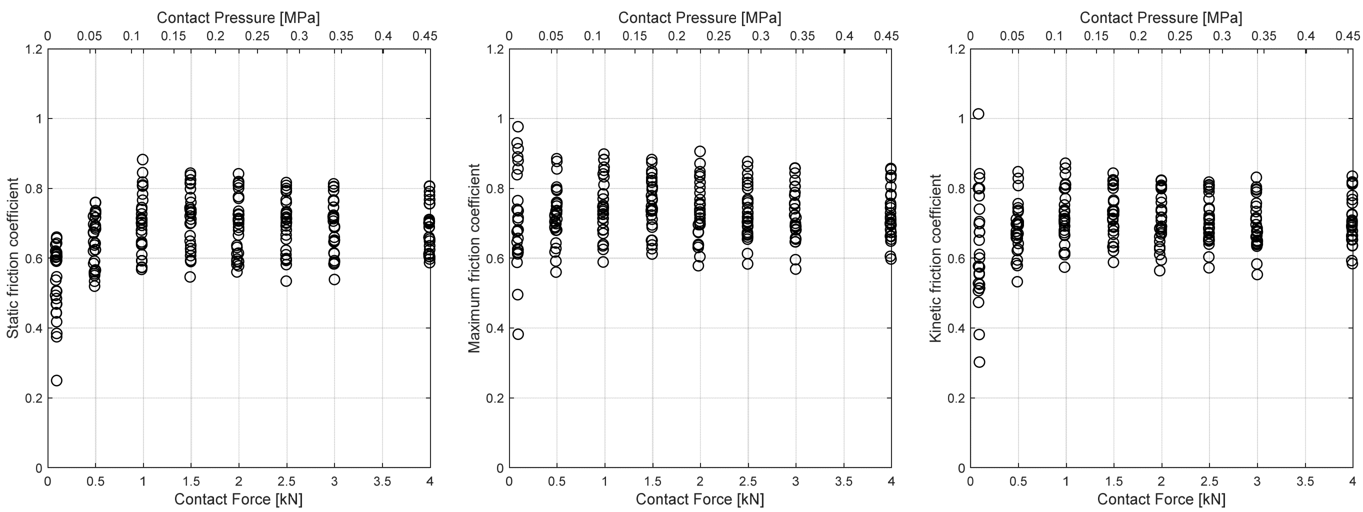

Fig. 5. Influence of the contact pressure on the friction coefficients of mortar-antique timber tests.

4.2 Mortar-modern timber

4.2.1 Mortar-modern planed timber

The mortar-modern planed timber tests yielded friction coefficients approximatively 20 % lower than the mortar-modern sawn timber (i.e., similar to the mortar-modern planed timber, or marginally higher), see Table 2. This decrease is solely attributable to the reduced surface roughness due to the different surface treatment, since the timber units are otherwise identical.

Table 2 shows that the contact pressure does not appear to influence the average of the friction coefficients for the wide range of contact pressures up to around 0.35 MPa of all tests. A different conclusion is reached with respect to the deviation from such average values. Table 2 disaggregates the static friction coefficients into low, intermediate, and high contact pressure (respectively $\sigma < 0.1$ MPa, 0.1 MPa $< \sigma < 0.2$ MPa, and $\sigma > 0.2$ MPa). For larger values of contact pressure, the static friction coefficient shows less variation. This observation is a general trend also for the maximum and kinetic friction coefficients, and for all mortar-timber test series. Therefore, the contact pressure contributes to reduce the variance.

4.2.2 Mortar-modern sawn timber

The friction coefficients obtained for the mortar-modern sawn timber units were the largest among all the materials considered in this study. They reached 0.84 for the average maximum friction coefficient and 0.79 for both the static and kinetic friction coefficients, see Table 2. The increase of approximately 25 % with respect to the mortar-modern planed timber tests is solely attributable to the larger surface roughness due to the different surface treatment sawn vs. planed.

The upper limit of normal pressures covered in these series was larger than the previous one, and detailed data inspection suggests that friction coefficients have a weak negative correlation with the contact pressure. However, this effect only occurs in the very high end of contact pressures (i.e., approximately for $\sigma > 0.3$ MPa), which is of limited relevance for practical applications.

4.3 Summary of Friction Coefficients

A summary of the mortar-timber friction coefficients (average and standard deviation) for the three types considered, and the three groups of normal contact pressure, is shown in Table 2. In addition to the observations in the previous sections, it can be seen that the static and kinetic coefficients are essentially very similar. Also, the difference between the static and the maximum friction coefficients is limited, which is compatible with a dry friction model. The values in Table 2 can be used to obtain the relevant fractile values for assessment or design of buildings with timber floor.

Table 2. Summary of friction coefficients for 87 mortar-timber tests.

Friction Coefficients Mortar-Timber		***Mortar – Modern Planed Timber***			***Mortar – Modern Sawn Timber***			***Mortar – Antique Timber***		
		Static	*Max*	*Kinetic*	*Static*	*Max*	*Kinetic*	*Static*	*Max*	*Kinetic*
Low contact pressure ($\sigma < 0.1$ MPa)	*Average*	0.63	0.67	0.63	0.79	0.84	0.79	0.62	0.74	0.68
	Standard Dev.	0.08	0.09	0.09	0.09	0.09	0.09	0.12	0.12	0.12
Intermediate contact pressure ($0.1 < \sigma < 0.2$ MPa)	*Average*	0.64	0.66	0.64	0.80	0.83	0.80	0.71	0.75	0.72
	Standard Dev.	0.06	0.06	0.06	0.07	0.07	0.07	0.09	0.08	0.07
High contact pressure ($\sigma > 0.2$ MPa)	*Average*	0.64	0.65	0.64	0.75	0.77	0.74	0.68	0.72	0.69
	Standard Dev.	0.04	0.04	0.03	0.07	0.08	0.07	0.07	0.07	0.06
All test units	***Average***	**0.63**	**0.66**	**0.64**	**0.77**	**0.81**	**0.77**	**0.67**	**0.73**	**0.70**
	Standard Dev.	0.06	0.07	0.07	0.08	0.09	0.08	0.10	0.09	0.09

5 Timber-timber Friction

5.1 Antique timber

Fig. 6(a) summarises the friction coefficients for the tests with antique timber units. They are slightly smaller than for the modern specimens with sawn finishing, see Table 3. This fact confirms the findings from the mortar-timber series (reduction is also of the order of 10-15 %), wherein an increased local roughness (with flat surface) seems to control over a more uneven surface but locally smooth.

Fig. 6(b) indicates a similar trend as for the mortar-antique timber tests: (i) a weak positive correlation between the friction coefficient and the contact pressure in the low pressure range ($\sigma < 0.1$ MPa), and (ii) an independence between these latter variables in the intermediate and high normal pressure range (and very high, up to almost $\sigma = 0.6$ MPa). The same comment applies to the maximum and kinetic friction coefficients.

5.2 Modern timber

Table 3 summarises the friction coefficients for the tests with contemporary construction timber units with planed and sawn surfaces. The values for planed units are strikingly lower compared to those for the rougher sawn units. The importance of the surface roughness, which has been noted to play a role in the mortar-timber series (20 % increase), hence appears to be greatly amplified when similar surfaces are in contact (100 % increase). For both surface treatments, the coefficients show a weak inverse correlation for higher normal pressures ($\sigma > 0.3$ MPa). Nevertheless, this range of normal pressure is not of interest for most practical applications.

5.3 Summary of Friction Coefficients

Table 3 presents a summary of the timber-timber friction coefficients (average and standard deviation) for the three types of test units considered, and the three groups of normal contact pressure. Contrary to mortar-timber tests, the kinetic coefficients are smaller than the static ones, which is aligned with classical descriptions of friction [7]. This is further confirmed by the fact that, for the large majority of the semi-cycles in these timber-timber tests, the static and the maximum friction coefficients coincided (see Table 3).

The comparison of Table 2 and Table 3 also shows that, except when the timber surface is extremely smooth (i.e., for planed timber), the timber-timber friction coefficients are roughly 15 % smaller than the corresponding mortar-timber values.

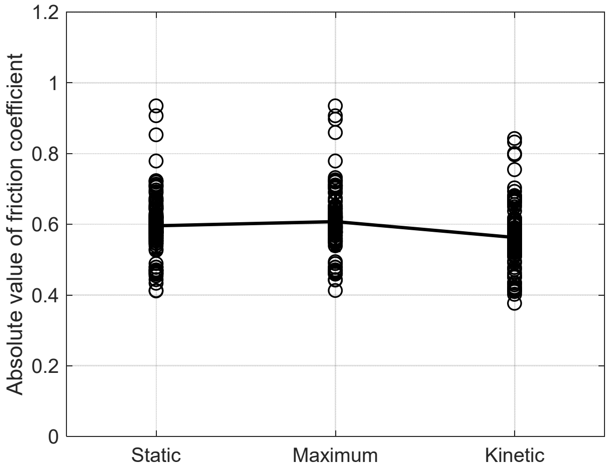

(a)

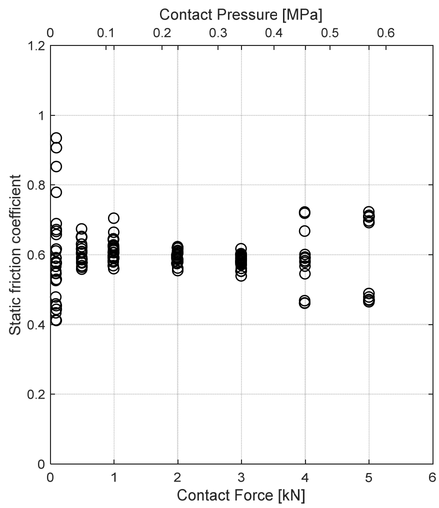

(b)

Fig. 6. Timber-timber friction tests of antique timber: (a) Friction coefficients for all semi-cycles; (b) Influence of the contact pressure on the static friction coefficient.

Table 3. Summary of friction coefficients for 100 timber-timber tests.

Friction Coefficients Timber-Timber		***Modern Planed Timber***			***Modern Sawn Timber***			***Antique Timber***		
		Static	*Max*	*Kinetic*	*Static*	*Max*	*Kinetic*	*Static*	*Max*	*Kinetic*
Low contact pressure (σ < 0.1 MPa)	*Average*	0.34	0.35	0.29	0.66	0.69	0.63	0.60	0.62	0.57
	Standard Dev.	0.10	0.10	0.08	0.09	0.10	0.10	0.11	0.11	0.10
Intermediate contact pressure (0.1 < σ < 0.2 MPa)	*Average*	0.33	0.34	0.30	0.69	0.69	0.65	0.61	0.61	0.57
	Standard Dev.	0.10	0.09	0.08	0.05	0.06	0.07	0.03	0.03	0.04
High contact pressure (σ > 0.2 MPa)	*Average*	0.31	0.31	0.27	0.66	0.66	0.62	0.59	0.59	0.56
	Standard Dev.	0.12	0.12	0.11	0.06	0.07	0.08	0.06	0.07	0.07
All test units	***Average***	**0.33**	**0.34**	**0.29**	**0.66**	**0.68**	**0.63**	**0.60**	**0.61**	**0.56**
	Standard Dev.	0.10	0.10	0.08	0.08	0.08	0.09	0.08	0.08	0.08

6 Influence of Specific Variables

This short section briefly discusses the effect of three additional parameters in the frictional response.

The influence of the cumulative loading on the frictional response was evaluated by performing several tests with repeated large-displacement cycles. This parameter was not found to affect the results since practically no strength degradation could be observed, even at relatively high values of contact pressure. As an example, Fig. 7 shows the results of mortar-modern sawn test at high level of contact pressure, $\sigma \approx 0.25$ MPa. Although it was not possible to carry out an exhaustive study on this variable due to time constraints, the previous conclusion was seen to be applicable to other combinations of test units as well.

During this experimental programme the effect of loading speed was also addressed. The applied default loading velocity was 0.1 mm/s, but tests at other speeds were also performed. Negligible differences were found for loading speeds between 0.01 mm/s and 2.5 mm/s. The latter value, which unfortunately is still much lower than the peak velocity demand expected from strong ground motions, was limited by geometrical constraints of the test setup and units.

Finally, tests with different combinations of grain directions between the timber units (parallel or perpendicular to each other) were performed. Distinct sliding directions with respect to the fibre orientation were also considered, including the case of mortar-timber tests. However, the observed differences were not statistically significant and therefore it was not possible to individuate this effect. A more extensive experimental programme focusing on this aspect can potentially overcome this difficulty.

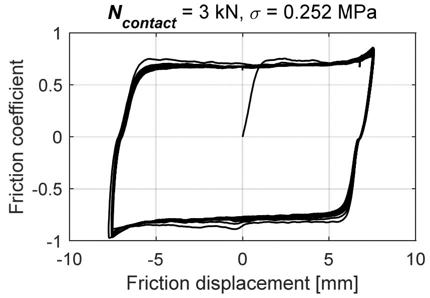

Fig.7. Effect of cumulative loading on frictional response of mortar-modern sawn timber tests, at high level of contact pressure.

7 Conclusions

The present study describes an experimental programme on cyclic friction tests to help characterizing the seismic response of timber floor to masonry wall connections in masonry buildings. After a literature review on dry wood friction and a differentiation of connection typologies between the pre-modern and the contemporary periods, a new setup for mortar-timber and timber-timber friction triplet tests was introduced. The units used in this study included timber from 16th century hand-hewn beams and two types of specimens representative of contemporary construction, namely with planed and rough sawn surfaces. The tests consisted in the application of cyclic shear displacements under different levels of contact pressure commonly expected in actual floor-wall connections. The experimental data are made publicly accessible through the Zenodo platform under the DOI: doi.org/10.5281/zenodo.3348328. The main conclusions were the following:

- Apart from those tests where friable mortar (representing antique mortar) was used, the test results can be adequately idealized by a frictional type of response, which is relevant for modelling purposes.
- The average static friction coefficient for the different materials varied between roughly 0.6 and 0.8, including both mortar-timber and timber-timber tests. Mortar-timber friction was approximately 15 % larger than timber-timber friction. The mentioned values are within those found in the literature, which typically oscillate between 0.15 and 0.9.
- An exception to the range indicated above was the timber-timber test results obtained with planed surface units, for which the average static friction coefficient was less than 0.35. Together with observations from the mortar-timber series, the influence of surface roughness appears to be a governing factor to increase friction resistance. In particular, an increased local roughness (with flat surface) predominates over a more uneven surface but locally smooth.
- The average kinetic and static friction coefficients were essentially similar for mortar-timber tests, while the expected reduction of the kinetic coefficient with respect to the static counterpart was only observed for the timber-timber tests.
- Larger contact pressures smoothed out some irregularity that could be observed in the force-displacement responses at lower levels of normal force. For some material combinations and high contact pressures ($\sigma > 0.3$ MPa), a weak negative correlation of the friction coefficients with normal pressure could be inferred. However, for practical applications it can be assumed that both variables are independent.
- The effect of cumulative loading, assessed by repeated large-displacement cycles, was found not to influence the response.
- Loading speed also did not affect the frictional behaviour, although higher velocity ranges, representative of seismic demands under strong ground motions, should be investigated.
- The values of the averages and standard deviations are provided in tables, which can be used by engineers to obtain characteristic and design values.

This experimental investigation is a small contribution to the significant research still needed to fully understand and characterize the seismic response of timber floor connections in masonry buildings. It provides friction coefficients for mortar-timber and timber-timber connections for the detailed seismic analysis of masonry buildings with timber floors.

Acknowledgments

This project was realised with the support by the Swiss Federal Office for the Environment, FOEN, in the framework of the action plan timber („Aktionsplan Holz") as well as by Lignum Holzwirtschaft Schweiz. Their support is gratefully acknowledged. The authors would also like to thank Dionysia Michalogianni for the help with the laboratory tests, and the availability and engagement of the laboratory technicians of the IIC-GIS Lab at EPFL, namely Serge Despont, Gérald Rouge, Gilles Guignet, and Sylvain Demierre.

Compliance with Ethical Standards

Funding: This project was realised with the support by the Swiss Federal Office for the Environment, FOEN, a government agency of Switzerland, in the framework of the action plan timber („Aktionsplan Holz") as well as by Lignum Holzwirtschaft Schweiz, a non-profit organisation of timber experts in Switzerland.

Conflict of Interest: The co-author Roland Brunner was employed by Lignum Holzwirtschaft Schweiz. The first author and both remaining co-authors have no conflicts of interest.

References

[1] Touliatos P.G., Seismic Behaviour of Traditionally-Built Constructions, in: P. V., S. M. (Eds.), Prot. Archit. Herit. Against Earthquakes, Int. Cent. Mech. Sci. (Courses Lect., Springer, Vienna, Austria, 1996: p. Vol. 359.

[2] Y. Nakamura, H. Derakhshan, G. Magenes, M.C. Griffith, Influence of Diaphragm Flexibility on Seismic Response of Unreinforced Masonry Buildings, J. Earthq. Eng. 21 (2017) 935–960. doi:10.1080/13632469.2016.1190799.

[3] I. Senaldi, G. Magenes, A. Penna, A. Galasco, M. Rota, The effect of stiffened floor and roof diaphragms on the experimental seismic response of a full-scale unreinforced stone masonry building, J. Earthq. Eng. 18 (2014) 407–443. doi:10.1080/13632469.2013.876946.

[4] P.B. Lourenço, L.S.F. Ramos, Characterization of Cyclic Behavior of Dry Masonry Joints, J. Struct. Eng. 130 (2004) 779–786. doi:10.1061/(ASCE)0733-9445(2004)130:5(779).

[5] A. Bernardini, C. Modena, M.R. Valluzzi, Load transfer mechanisms in masonry: Friction along a crack within a brick, Mater. Struct. 31 (1998) 42–48.

[6] T. Zimmermann, A. Strauss, K. Bergmeister, Structural behavior of low- and normal-strength interface mortar of masonry, Mater. Struct. 45 (2012) 829–839.

[7] R. Steiger, G. Fink, S. Nerbano, E. Hack, K. Beyer, Experimental investigation of friction stresses between adjacent panels made of Oriented Strand Board (OSB) and between OSB panels and glued laminated timber (GLT) frame members, Mater. Struct. 51 (2018) 1–14. doi:10.1617/s11527-017-1124-5.

[8] J.R. Aira, F. Arriaga, G. Íñiguez-González, J. Crespo, Static and kinetic friction coefficients of Scots pine (Pinus sylvestris L.), parallel and perpendicular to grain direction, Mater. Construcción. 64 (2014) 1–9. doi:10.3989/mc.2014.03913.

[9] S. Chen, F. Hsu, Frictional Properties of Wood Flooring Materials, Taiwan J. For. Sci. 20 (2005) 95–104.

[10] M. Xu, L. Li, M. Wang, B. Luo, Effects of Surface Roughness and Wood Grain on the Friction Coefficient of Wooden Materials for Wood-Wood Frictional Pair, Tribol. Trans. 57 (2014) 871–878. doi:10.1080/10402004.2014.920064.

[11] Q. Meng, T. Hirai, A. Koizumi, Frictional Coefficients between Timber and Some Structural Sheet Materials, Mokuzai Gakkaishi. 54 (2008) 281–288. doi:10.2488/jwrs.54.281.

[12] W.M. McKenzie, H. Karpovich, The frictional behaviour of wood, Wood Sci. Technol. 2 (1968) 139–152. doi:10.1007/BF00394962.

[13] B.A. Svensson, S. Nyström, P.A. Gradin, H. Höglund, Frictional testing of wood-Initial studies with a new device, Tribol. Int. 42 (2009) 190–196. doi:10.1016/j.triboint.2008.03.009.

[14] M. Seki, H. Sugimoto, T. Miki, K. Kanayama, Y. Furuta, Wood friction characteristics during exposure to high pressure: influence of wood/metal tool surface finishing conditions, J. Wood Sci. 59 (2013) 10–16.

[15] K. Platzgummer, F. Vanin, K. Beyer, A Review of the Building Typologies and Structural Details of Stone Masonry Buildings in Basel, Lausanne, Switzerland, 2015.

[16] V.L. Popov, Contact Mechanics and Friction: Physical Principles and Applications, 2010.

[17] D. Atack, D. Tabor, The friction of wood, Proc. R. Soc. London. A246 (1958) 539–555.

[18] S.V. Glass, S.L. Zelinka, Chapter 4: Moisture Relations and Physical Properties of Wood, in: F.P. Laboratory (Ed.), Wood Handb., Madison, USA, 2010.

[19] L. Bejo, E.M. Lang, T. Fodor, Friction coefficients of wood-based structural composites, For. Prod. J. 50 (2000) 39–43.

[20] P. Niemz, Physik des Holzes und der Holzwerkstoffe, Leinfelden- Echterdingen, Germany, 1993.

[21] Y. Murase, Friction of wood sliding on various materials, J. Fac. Agric. Univ. 28 (1984) 147–160.

[22] S. Zhang, N. Richart, K. Beyer, Numerical evaluation of test setups for determining the shear strength of masonry, Mater. Struct. 51 (2018) 1–12. doi:pre-print: http://infoscience.epfl.ch/record/252996?ln=en.

[23] J.R. Riddington, K.H. Fong, P. Jukes, Numerical study of failure initiation in different joint shear tests, Mason. Int. 11 (1997) 33–64.

[24] BAFU, Qualitätskriterien für Holz und Holzwerkstoffe im Bau und Ausbau. Handelsgebräuche für die Schweiz., Zurich, Switzerland, 2010.

[25] EN 14080:2013, Timber structures - Glued laminated timber and glued solid timber - Requirements, 2013.

[26] EN 14081-1:2005+A1:2011, Timber structures – Strength graded structural timber with rectangular cross section – Part 1: General requirements, 2011.

[27] The MathWorks Inc., MATLAB - Version R2016b, (2016).